

## AN ACTIVE-RC RECONFIGURABLE LOWPASS-POLYPHASE TOW-THOMAS BIQUAD FILTER

Akira Yamazaki<sup>1</sup>, Arun Ravindran<sup>2</sup>, Omer Can Akgun<sup>1</sup> and Mohammed Ismail<sup>1</sup>

<sup>1</sup>Analog VLSI Lab, Department of Electrical Engineering  
The Ohio State University, Columbus, Ohio 43210

<sup>2</sup>Department of Electrical and Computer Engineering  
University of North Carolina at Charlotte, Charlotte, NC 28223

**Abstract-** A novel active-RC biquad is presented which can be reconfigured as a polyphase filter for a low IF wireless receiver architecture, and as a lowpass filter for a zero IF wireless receiver architecture. A second order lowpass-polyphase reconfigurable filter is implemented to illustrate the technique. A 1.8V fully differential operational amplifier in 0.18 $\mu$ m CMOS technology is used as the active element.

### 1. INTRODUCTION

The proliferation of wireless standards has resulted in a demand for integrated wireless receivers capable of multi-standard operation using the same hardware. While zero-IF (intermediate frequency) receiver architectures are free from the problem of image frequencies [1], they suffer from issues such as DC offsets, flicker noise etc. in CMOS implementations. On the other hand, low-IF architectures require image rejection, but are relatively free from DC offsets and flicker noise. To enable operation across multiple wireless standards, a low IF – zero IF reconfigurable wireless receiver architecture can be used [2], where the low IF architecture is used for narrow channel standards, and zero IF architecture for wide channel standards. Such a receiver requires a reconfigurable analog baseband filter that serves as a channel select lowpass filter for zero IF, and image reject/channel select polyphase filter for the low IF architecture.

In [3-5], a fifth order polyphase Butterworth transfer function is realized by cascading first order polyphase sections. The circuit presented in [3-5] cannot be easily reconfigured to realize the complex conjugate poles required for the lowpass filter. In this paper, we present a novel active-RC biquad that can be easily reconfigured to implement both lowpass and polyphase filters.

The paper is organized as follows. In the next section, a brief review of active polyphase filters is presented. The following section describes the operation of the proposed reconfigurable polyphase-lowpass biquad. Details of the circuit implementation using a 1.8V fully differential CMOS operational amplifier (Opamp) are then presented. Simulation results verify the operation of the proposed biquad. The paper concludes with a summary of presented results and possible applications in commercial wireless receivers.

### 2. ACTIVE POLYPHASE FILTERS

To motivate the development of an active polyphase filter, we examine the low-IF wireless receiver architecture with respect to image rejection. After quadrature downconversion from the RF to IF frequency, the signal and its image can be considered to have positive and negative components as shown in Fig.1 [4]. This suggests that a filtering operation that has a pass band in the positive signal frequencies, and a stop band in the negative signal frequencies, could serve to achieve both image rejection and channel selection. Such an asymmetrical filtering operation requires the use of polyphase filter because real filters have symmetrical response for negative and positive frequencies.

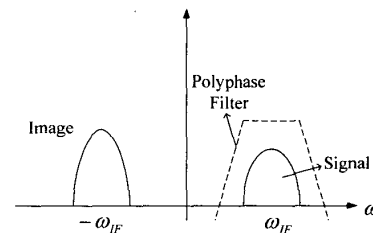


Fig.1 Signal and image after quadrature downconversion

In order to realize the polyphase filtering operation, poles of a low pass filter are shifted by  $\omega_c$ , where  $\omega_c = \omega_{IF}$ , is the center frequency of the polyphase filter.

Mathematically,

$$H(j\omega) \rightarrow H(j\omega - j\omega_c) \quad (1)$$

where  $H(j\omega)$  represents the s-domain transfer function of the real filter. In conventional analog signal processing, the operation described by (1) cannot be realized using real physical components. However, in a wireless receiver, the outputs of the quadrature I-Q paths are complex conjugates of each other, making it possible to implement a polyphase analog filter.

In one such approach [3-5], a single complex pole is synthesized from a real pole using the following transformations,

$$H_{lp}(j\omega) = \frac{1}{1 + j\omega/\omega_0} \quad (2)$$

$$H_{pp}(j\omega) = \frac{1}{1 - j\omega_c/\omega_0 + j\omega/\omega_0} \quad (3)$$

where  $\omega_0$  is the cut-off frequency of the filter.

An Opamp-RC realization of a single complex pole and corresponding pole locations in the s-plane are shown in Fig. 2 [4]. Higher order filters are synthesized by cascading first order sections. Note that implementing a lowpass filter using the circuit presented in Fig. 2, requires extensive reconfiguration to synthesize conjugate poles. This motivates the development of a biquad capable of readily realizing both conjugate and non-conjugate pole pairs.

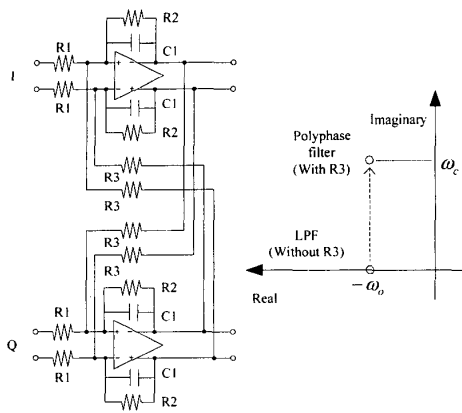


Fig.2 First order polyphase filter and pole location

### 3. RECONFIGURABLE BIQUAD

To develop a reconfigurable lowpass-polyphase biquad, we first examine the transfer function of a real low pass biquad,

$$H(s) = \frac{-\omega_0^2}{s^2 + \omega_0 s/Q + \omega_0^2} \quad (4)$$

where  $\omega_0$  is the cut-off frequency of the filter and  $Q$  is the filter  $Q$ -factor. As shown in Fig. 3, (4) can be implemented using well known state variable synthesis techniques using two inverting integrators and an inverter [6-7]. A Tow-Thomas state variable filter biquad, shown in Fig.4, is used to illustrate this technique.

Applying the polyphase transformation described by (1) to (4), we have

$$H(s - s_c) = \frac{-\omega_0^2}{(s - s_c)^2 + \omega_0(s - s_c)/Q + \omega_0^2} \quad (5)$$

where  $s_c = j\omega_c$ , is the polyphase filter center frequency.

Fig. 5 shows the use of the state variable techniques to realize a polyphase filter using a complex integrator. A lossless complex integrator can be realized from the circuit shown in Fig.2, by removing the feedback resistor  $R_2$ . The polyphase Tow-Thomas biquad is shown in Fig. 6, where fully differential Opamps are used as the active elements. Note that by using fully differential Opamps, the inverter at the last stage of Fig. 4 can be removed. The filter center frequency, cutoff frequency,  $Q$  factor and DC gain are given by

$$\omega_c = \frac{1}{R_c C_f} \quad (6)$$

$$\omega_0 = \frac{1}{R_w C_f} \quad (7)$$

$$Q = \frac{R_q}{R_w} \quad (8)$$

$$A_v = \frac{-R_w}{R_i} \quad (9)$$

In order to reconfigure this filter as a lowpass biquad,  $R_c$  is opened using the switch  $sw$  placed in series with  $R_c$ . This converts the complex integrator into a real integrator. The remaining elements remain unchanged. Implementation of resistors  $R_c$ ,  $R_q$  and  $R_w$  using circuit elements such as triode region MOSFETs, and the feedback capacitor  $C_f$  using programmable capacitor arrays, enables tuning and programming of the cutoff frequencies and  $Q$  factors of the two filter configurations.

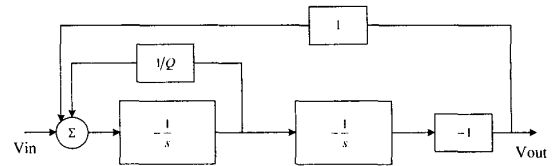


Fig.3 State variable realization of a real biquad

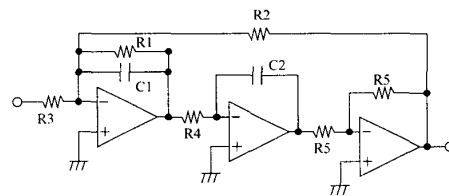


Fig.4 The Tow-Thomas biquad

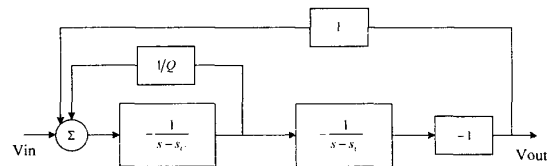


Fig.5 State variable realization of a polyphase biquad

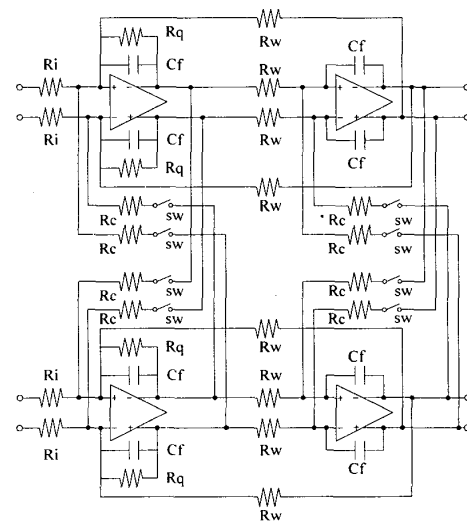


Fig.6 Polyphase-Lowpass reconfigurable Tow-Thomas biquad

#### 4. CIRCUIT IMPLEMENTAION

To realize the reconfigurable biquad as shown in Fig. 6, fully differential Opamps with high open loop gain, large bandwidth and low output resistance is required. To achieve the above-mentioned requirements, as seen in Fig. 7, a fully differential three stage design is used. The Opamp has a differential first stage, a common-source second stage and a source follower third stage. The first two stages realize high open loop gain, while the third stage buffers the output. Note that common mode feedback is applied to stabilize the common mode voltage levels V1 and V2 at the output of the second stage. In the remainder of this section, expressions are developed for the gain and pole locations of the Opamp of Fig 7. Due to symmetry of operation, only one-half of the circuit is analyzed.

Since resistors  $R_i$ ,  $R_c$  and  $R_w$  in Fig.6 are connected to the input of the Opamp, a low input capacitance is required to obtain large bandwidth. By adding cascode devices M3/M4 to the input stage, the Miller effect due to parasitics associated with transistors M1 and M2 is significantly reduced. The input pole  $\omega_{in}$  can be estimated as

$$\omega_{in} \approx -\frac{1}{R_{in}(C_{GS1} + 2C_{GD1})} \quad (10)$$

where  $C_{GS1}$  and  $C_{GD1}$  are the intrinsic gate-source and gate-drain capacitance of M1, and  $R_{in}$  is the resistor connected to the Opamp input in the filter implementation of Fig. 6.

The small signal gain of the first stage  $A_1$  is given by

$$|A_1| \approx g_{m1}(r_{o5} \parallel g_{m3}r_{o3}r_{o1}) \quad (11)$$

where  $g_{m1/3}$  and  $r_{o1/3}$  are transconductance and output resistance of transistors M1 / M3 respectively. The dominant pole  $\omega_1$  can be expressed as

$$\omega_1 \approx -\frac{1}{(r_{o5} \parallel g_{m3}r_{o3}r_{o1}) |A_2| C} \quad (12)$$

where C is the compensation capacitance and  $A_2$  is the small signal gain of the second stage.

$$|A_2| \approx g_{m7}(r_{o7} \parallel r_{o9}) \quad (13)$$

The second pole  $\omega_2$  associated with the output of the second stage can be approximated as,

$$\omega_2 \approx -\frac{1}{(r_{o7} \parallel r_{o9} \parallel 1/g_{m7})(C_{GD9} + C_{GD13})} \quad (14)$$

Assuming  $g_{m13} \ll R_w, R_q, R_c$  the output pole  $\omega_{out}$  is given by

$$\omega_{out} \approx -\frac{1}{(1/g_{m13})C_f} \quad (15)$$

where  $C_f$  is the feedback capacitor of Fig. 6.

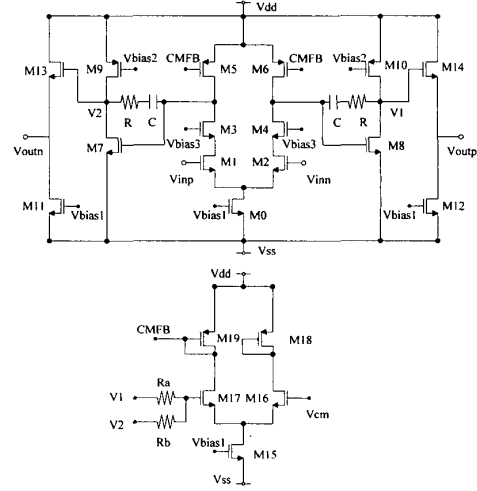


Fig.7 Fully differential operational amplifier

From the above equations, we note that large values for  $g_{m7}$  and  $g_{m13}$ , pushes the second and output poles to higher frequencies while lowering the output resistance. Moreover the left half plane zero, introduced by the series compensation resistor R, improves the phase margin of the system.

#### 5. SIMULATION RESULTS

The proposed reconfigurable biquad of Fig.6 was implemented using the fully differential Opamp of Fig. 7. The circuit was simulated at a supply of 1.8V, using 0.18 $\mu$ m CMOS models. The threshold voltages of the NMOS and PMOS are 0.35V and 0.4V respectively. The biquad was designed to implement a Butterworth polynomial for a center frequency  $\omega_c = 2$  MHz and cutoff frequency  $\omega_o = 500$  KHz in the polyphase mode and cutoff frequency  $\omega_o = 7.5$ MHz in the lowpass mode. Small signal models were constructed to determine the Opamp performance requirements. The primary Opamp specifications were 60 dB DC gain, 35 MHz unity gain bandwidth, and a phase margin of 60 degrees while driving a 105k $\Omega$  resistive load and a 3pF capacitive load.

Table 1 shows the RC values of the filter for the two modes of operation.

Table 1. RC component values

| RC Value | Low pass filter                            | Polyphase filter                           |
|----------|--------------------------------------------|--------------------------------------------|
|          | $\omega_c = 0$ MHz<br>$\omega_o = 7.5$ MHz | $\omega_c = 2$ MHz<br>$\omega_o = 500$ KHz |
| Ri       | 5.3 k $\Omega$                             | 26 k $\Omega$                              |
| Rw       | 21 k $\Omega$                              | 105 k $\Omega$                             |
| Rq       | 14.8 k $\Omega$                            | 74 k $\Omega$                              |
| Rc       | open                                       | 26.5 k $\Omega$                            |
| Cf       | 1 pF                                       | 3 pF                                       |
| R        | 3 k $\Omega$                               | 4.5 k $\Omega$                             |
| C        | 2.6 pF                                     | 3.2 pF                                     |

Fig.8 shows the frequency response of the polyphase biquad for different closed loop gains obtained by tuning the resistor  $R_c$ . An image attenuation of more than 33 dB is achieved at -2 MHz.

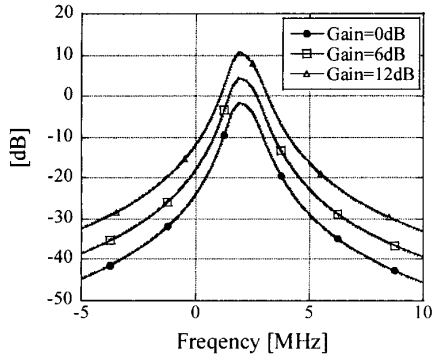


Fig.8 Polyphase filter frequency response

Fig.9 shows the frequency response of the lowpass biquad for different Q factors obtained by tuning the resistor  $R_q$ .

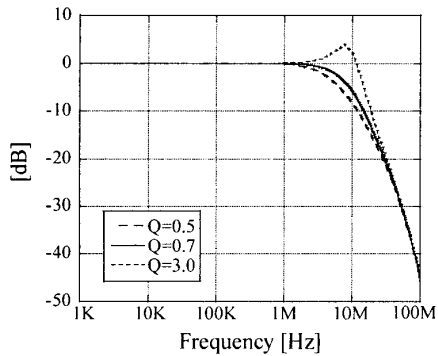


Fig.9 Lowpass filter frequency response

The third order input intercept (IIP3) for both polyphase and lowpass modes are shown in Fig. 10. For the in-band IIP3, a two tone test was performed with the tones at 1.9 MHz and 2.1 MHz while for the out-of-band IIP3, the tones were set at 10 MHz and 22MHz. The filter performance specifications for the two modes of operation are summarized in Table 2.

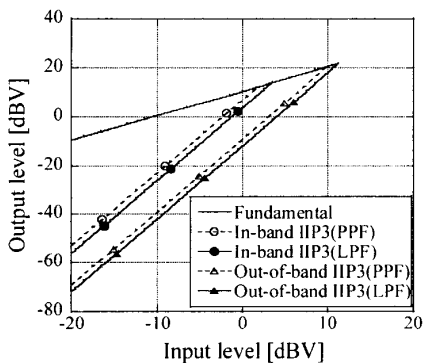


Fig. 10 In-band and Out-of-band IIP3

Table 2. Simulated reconfigurable biquad parameters

|                            | Low pass biquad                            | Polyphase biquad                           |
|----------------------------|--------------------------------------------|--------------------------------------------|
|                            | $\omega_c = 0$ MHz<br>$\omega_o = 7.5$ MHz | $\omega_c = 2$ MHz<br>$\omega_o = 500$ KHz |
| Gain                       | 0-12dB                                     | 0-12dB                                     |
| Q                          | 0.5-3.0                                    | 0.5-3.0                                    |
| In-band IIP3               | 3.3dBV                                     | 1.7dBV                                     |
| Out-of-band IIP3           | 11.2dBV                                    | 9.8dBV                                     |
| Input referred noise (rms) | -73dBV                                     | -67.5dBV                                   |
| Power                      | 14.4mW                                     | 14.4mW                                     |

## 6. CONCLUSIONS

A new active-RC implementation of a reconfigurable polyphase – lowpass filter based on a Tow-Thomas biquad is presented. The proposed filter has independent tuning of DC gain, the cut-off frequency, Q factor and center frequency for both the polyphase and lowpass modes of operation. Simulation results for the biquad, implemented in 0.18 $\mu$  CMOS technology, suggest possible utility in realizing a Bluetooth- 802.11b multi-standard wireless receiver analog baseband chain.

## 7. REFERENCES

- [1] B. Razavi, "RF Microelectronics", Prentice-Hall Inc., Upper Saddle River, NJ, 1998.
- [2] A. Savla, A. Ravindran and M. Ismail, "A Reconfigurable Low-IF/Zero-IF Receiver Architecture for Multi-Standard Wide Area Wireless Networks", *ICECS 2003*, pp. 934-937, December 2003.
- [3] J. Crols, and M. Steyaert, "An analog integrated polyphase filter for a high performance low-IF receiver," *Proc. Symp. VLSI Circuits Tech., Dig.*, 1995, pp. 87-88.
- [4] J. Crols, and M. Steyaert, "Low-IF topologies for high-performance analog front ends of fully integrated receivers," *IEEE. Trans. Circuits and Systems-II, Analog and Digital Signal Processing*, vol. 45, pp. 269-282, March 1998.
- [5] T. Cho, D. Kang, S. Dow, C. H. Heng, and B. S. Song, "A 2.4GHz Dual-Mode 0.18 $\mu$ m CMOS Transceiver for Bluetooth and 802.11b," *ISSCC Digest of Technical Papers*, pp. 88-89, Feb. 2003.
- [6] A. Sedra and P. Brackett, "Filter Theory and Design : Active and Passive," Matrix Publication Inc., Portland , 1978.
- [7] R. Schaumann and V. Valkenburg, "Design of Analog Filters," Oxford University Press, 2001.